Exp Brain Res (2006) 172: 370–386
DOI 10.1007/s00221-005-0334-1

RESEARCH ARTICLE

Peter Melzer · Gregory C. Champney
Mark J. Maguire · Ford F. Ebner

Rate code and temporal code for frequency of whisker stimulation in rat primary and secondary somatic sensory cortex

Received: 26 July 2005 / Accepted: 6 December 2005 / Published online: 3 February 2006

Abstract We recorded responses to frequencies of whisker stimulation from 479 neurons in primary (S1) and secondary (S2) somatic sensory cortex of 26 urethane-anesthetized rats. Five whiskers on the right side of the snout were deflected with air puffs at seven frequencies between 1 and 18/s. In left S1 (barrels and septa) and S2, subsets of neurons (5%) responded to whisker stimulation across the entire range of frequencies with ≥1 electrical discharges/ten stimuli (*full responders*). In contrast, 60% of the recorded cells responded above threshold only at stimulus frequencies below 6/s and 35% remained subthreshold at all frequencies tested. Thus, the *full responders* are unique in that they were always responsive and appeared particularly suited to facilitate a dynamic, broadband processing of stimulus frequency. *Full responders* were most responsive at 1 stimulus/s, and showed greatest synchrony with whisker motion at 18 stimuli/s. The barrel cells responded with the greatest temporal accuracy between 3 and 15 stimuli/s. The septum cells responded less accurately, but maintained their accuracy at all frequencies. Only septum cells continued to increase their discharge rate with increasing stimulus frequency. The S2 cells discharged with lowest temporal accuracy modulated only by stimulus frequencies ≤ 6/s and exhibited the steepest decrease in discharge/stimulus with increasing stimulus frequency. Our observations suggest that *full responders* in the septa are well suited to encode high frequencies of whisker stimulation in timing and rate of discharge. The barrel cells, in contrast, showed the strongest temporal coding at stimulus frequencies in the middle range, and S2 cells were most sensitive to differences in low frequencies. The ubiquitous decline in discharge/stimulus in S1 and S2 may explain the decrease in blood flow observed at increasing stimulus frequency with functional imaging.

Keywords Vibrissa · Stimulus frequency · Single units · Barrel · S1 and S2 cortex

P. Melzer (✉) · G. C. Champney · M. J. Maguire · F. F. Ebner
Department of Psychology, Vanderbilt University, 301 Wilson Hall, 111 21st Ave. S, Nashville, TN 37203, USA
E-mail: peter.melzer@vanderbilt.edu
Tel.: +1-615-3437614
Fax: +1-615-3223228

Introduction

Rats use their mystacial whiskers, i.e., the sensory sinus hairs on the snout, to actively palpate their environment with periodic whisks (Vincent 1912; Welker 1964). The mystacial whiskers are represented topographically in primary somatic sensory cortex by neural aggregates called "barrels" (Woolsey and Van der Loos 1970). Neurons in barrel cortex can differentiate between active whisker movements and whisker contact (Kleinfeld et al. 2002). The frequency with which whiskers are moved thus appears to play a fundamental role in whisker touch (Hutson and Masterton 1986; Carvell and Simons 1990, 1995; Ahissar et al. 1997; Harris and Diamond 2000; Krupa et al. 2001, 2004; Berg and Kleinfeld 2003), and the whisker-to-barrel pathway may be superbly suited to examine the neural code of stimulus frequency in the somatic sensory pathway.

In primate primary somatic sensory cortex, Mountcastle et al. (1967, 1969) observed that the frequency of vibrotactile stimulation of the glabrous skin of the hand might be encoded by the inter-spike interval of rapidly adapting neurons. However, these authors could not rule out that stimulus frequency may be encoded in neural discharge rate, and evidence has been provided that the code may be different in primary and secondary somatic sensory cortex (Salinas et al. 2000; Romo et al. 2002). A comparison of neural responses in the two cortical areas to different frequencies of whisker stimulation has not been reported for the rat, though primary somatic sensory (Ahissar and Kleinfeld 2003; Arabzadeh et al. 2003) and primary motor cortex (Kleinfeld et al. 2002) have been

examined. The present study was designed to fill this gap. Preliminary results have been published in abstract form (Champney et al. 2001).

Material and methods

Animals

Twenty-six adult female or male Long-Evans rats >2 months of age (350–550 g b.w.) were used in this study. The animals were obtained from an in-house breeding colony where they were raised in standard cages in a 12:12 light/dark cycle with access to food and water ad libitum. All methods were approved by the Vanderbilt University Animal Care Committee and were in accordance with NIH-approved guide lines.

Single-unit recordings

The rats were anesthetized with intraperitoneal injections of 30% urethane (1.5 g/kg b.w.). Body temperature was maintained at 37°C with a heating pad. A craniotomy was made over the left hemisphere, the dura was opened, and whisker representations in primary (S1) and secondary (S2) somatic sensory cortex were mapped with single-unit recordings using single epoxylite-coated tungsten wire microelectrodes (length 80 mm, impedance 2 MΩ, tip $\varnothing < 1$ μm; Micro Probe Inc., Potomac, MD). A hand-held probe was used to identify the whisker that produced the most vigorous neural responses (principal whisker). The mystacial whiskers of rats and mice are arrayed in five rows named A–E from dorsal to ventral (Woolsey and Van der Loos 1970). They are numbered in rising order beginning with one at the caudal end. Four whiskers, called straddlers, are positioned between the rows at the caudal end and are labeled α (dorsal) to δ (ventral). Mapping of neural receptive fields reveals two separate topographic whisker representations, one in S1 and the other in S2 cortex (Woolsey and Van der Loos 1970; Carvell and Simons 1986). After the two whisker maps had been located in the present study, one array of four microelectrodes (~200 μm apart; Frederic Haer & Co., Bowdoinham, ME) was lowered ~350 μm perpendicular to the pial surface into each whisker map.

The recording depths of neural responses to whisker stimulation were determined with the micrometer readings on the microelectrode drives. The depth at which the electrodes contacted the cortical surface was taken as zero. Dimpling of the surface was avoided by retracting the electrodes ~50 μm after the initial penetration of cortex. Spontaneous neural discharge was collected at each site for 2 min. Then, neural responses were recorded during 1-min epochs while 30-ms air puffs were used to stimulate multiple whiskers at seven frequencies up to 18/s. Single-units were discriminated online using a window discriminator (Bak Electronics, Mount Airy, MD) and off-line using a multi-channel spike data acquisition processor (Plexon Inc., Dallas, TX). After recording at ~350 μm, the microelectrode arrays in S1 and S2 were advanced roughly 100 μm three times and sets of data were collected at each depth. At the end of the recording session the rats were euthanized and processed for histology.

The stimulus

On average five whiskers were deflected with 1, 18, 3, 15, 6, 12 and 9 air puffs/s (*apps*). The spectrum of stimulus frequencies was chosen to cover the whisk rates that alert rats are known to utilize during idle whisking (~5 whisks/s; Gao et al. 2001), exploration (6–9 whisks/s; Carvell and Simons 1990, 1995; Fee et al. 1997), and object discrimination (13–20 whisks/s; Hutson and Masterton 1986; Carvell and Simons 1995; Mineo et al. 2002; Berg and Kleinfeld 2003). The air puffs were produced by compressed air (up to 24 kPa) delivered through tubing and toggled with a solenoid that was triggered by a pulse generator (James Long Co., Caroga Lake, NY). The trigger signals for the solenoid were recorded as time stamps for stimulus onset. Because of the length of the air hose, the onset of the whisker deflections was delayed by 26 ms and this delay was subtracted from the onset of all evoked neural responses. The 2-mm hose opening was positioned at ~60° angle ~30 mm above the plane of the whisker rows to deflect them approximately 3 mm at mid-length ventro-caudally at 0.7°/ms. The jet was directed to include the previously identified principal whiskers and surround whiskers evenly.

Examples of the time courses of air puffs recorded with a pressure transducer (James Long Co., Caroga Lake, NY) at the muzzle of the hose are shown in Fig. 1. At frequencies ≤ 6 *apps*, the baseline-to-peak pressure change was stable at 13 ± 1 kPa and the shapes of the pulses remained unaltered. In contrast, at frequencies ≥9 *apps* the period of time available for dissipation of air was abbreviated by the onset of the subsequent puff and the air pressure did not return to baseline. A modulated, continuous stream of air was released on the whiskers producing a ramp-and-hold stimulus perhaps similar to "flutter" (Mountcastle et al. 1967, 1969). However, even the smallest baseline-to-peak pressure difference (10 kPa at 18 *apps*) was large enough to deflect the whiskers with sufficient velocity and amplitude to drive cortical responses (Kleinfeld et al. 2002).

Data analysis

The data files with the waveforms of the recorded action potentials and the stimulus time stamps were concatenated and neural discharges were re-discriminated and sorted off-line according to waveform using principal components and cluster cutting in Offline Sorter (Plexon

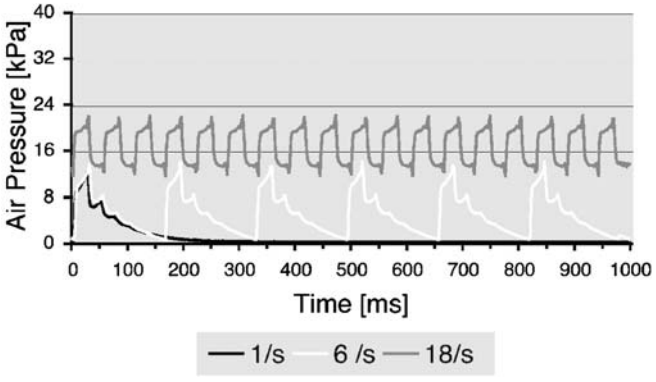

Fig. 1 Pressure curves of air puffs used for whisker stimulation. Curves for 1 (*black line*), 6 (*white line*) and 18 (*gray line*) air puffs/s (*apps*) are shown as examples. The pressure of the air puffs averaged over 60 s is plotted against time after onset. At the high frequency, the decrease in air pressure was cut short by the advent of the next air puff producing a "flutter" rather than a train of discrete pulses

Inc., Dallas, TX). Briefly, the first two principal components of the waveforms were displayed in Cartesian coordinates on a computer monitor and boundaries were drawn and redrawn around the clusters of data points by one investigator (G.C.C.) until complete separation of the waveforms was accomplished. Using Neuroexplorer (Nex Technologies, Littleton, MA), single-unit peri-stimulus raster plots, peri-stimulus time histograms and latency histograms were constructed at 2-ms binning at each frequency of whisker stimulation. Bursts of neural discharge were quantified with a simplified analysis developed by Gopal and Gross (1996) using two discharges as the minimum number constituting a burst and surprise level 3.

In addition, autocorrelograms were constructed for each neuron at each stimulus frequency using the method of Perkel et al. (1967) at 2-ms binning and ± 0.5 s window width (details are described at: http://www.mulab.physiol.upenn.edu/crosscorrelation.html). The arithmetic means of the coincidences were plotted for the three locations examined. Coincidences were absent at time 0. Owing to limits in printing resolution the resulting gap is not always detectable in the histograms. The counts per bin on both sides adjacent to 0 constitute the responses to stimuli of same order, i.e., the responses to the first stimulus were matched with the responses to the first and, at >1 stimulus/s, those to the second were matched with those to the second and so forth. They were taken to form one peak whose width at half distance between the maximum and the baseline (full width half maximum or FWHM) was used to represent the temporal accuracy with which the neurons responded to stimulation. The fewer the bins in which the coincidences accumulated, the narrower the peak and the greater the temporal accuracy of the response, i.e., the more the cells responded to the stimulus in a precisely timed, reproduced fashion commensurate with stimulus frequency.

The mean spontaneous discharge per second was subtracted from the discharge per second recorded with whisker stimulation to determine stimulus-related discharge rates. Analogous to the assessment of discharge per stimulus recorded from auditory (Rose et al. 1971) and somatic sensory (Johnson 1974) primary afferents, we examined the efficacy of neural responsiveness at low (1 *apps*), intermediate (6 *apps*) and high frequencies of stimulation (18 *apps*). No cell was found that responded with ≥ 0.5 discharge/stimulus at 18 *apps*. However, a select number of cells responded with more than one discharge per ten stimuli above their spontaneous rates at the three frequencies tested providing the capability of conveying tactile information over a wide range of stimulus frequencies.

Histology

The euthanized rats were transcardially perfused with 0.1 M phosphate-buffered saline followed by 2% paraformaldehyde in 0.1 M phosphate-buffered saline. The brain was removed, post-fixed in the same fixative at 5°C for 12 h, then immersed in 30% sucrose in 0.1 M phosphate-buffered saline and stored at 5°C until sectioning. Before sectioning, the cortical hemispheres were separated from the brainstem and flattened. Forty micron-thick sections were cut parallel to the surface at -20°C on a sliding microtome and stained for cytochrome oxidase activity (Wong-Riley 1979). In these preparations, the barrels in S1 cortex were clearly distinguishable as dark patches separated by the lightly stained septa (Fig. 2). The recording sites formed roughly linear arrays of four evenly spaced marks that could be allocated to barrels and septa in S1. In S2, no morphological landmarks were discernible and, therefore, the sites were mapped in reference to the A row barrels in S1.

Results

In total, recordings were collected from 479 neurons responsive to whisker stimulation in primary (S1) and secondary (S2) somatic sensory cortex. Sixty percent of these neurons discharged at least once per ten stimuli above spontaneous activity at one of the stimulus frequencies tested. The average response of all neurons decreased non-linearly with increasing frequency of whisker stimulation, i.e., 53% of the total population responded above threshold at 1 *apps*, 27% at 6 *apps* and a mere 7% were responsive at 18 *apps*. Thirty-three percent of the total was responsive to whisker stimulation only at 1 *apps*, 7% responded only at 6 *apps* and 0.6% responded only at 18 *apps* (Table 1). Fourteen percent of all cells were responsive to 1 and 6 *apps* and only 6% responded above threshold across the entire range of stimulus frequencies.

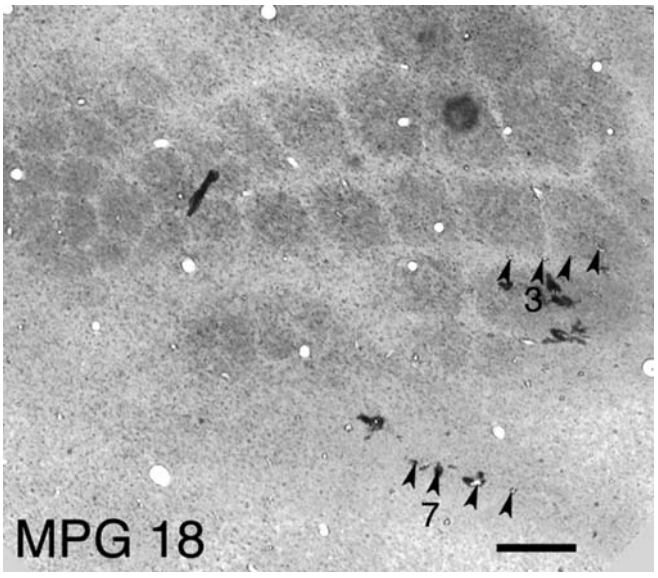

Fig. 2 Recording sites in a typical histological preparation. The micrograph was taken from a 40 μm-thick section cut parallel to the pia through flattened cortex of rat MPG 18 and stained for cytochrome oxidase activity. The *densely stained patches* are barrel centers. Electrode penetration sites are recognizable as rows of four evenly spaced *dark brown annuli*. The *arrowheads* point at the loci of electrode penetrations 1–4 in S1 (*penetration 3 is labeled*) and 5–8 in S2 cortex (*penetration 7 is labeled*). Orientation: rostral is *left* and medial is *up*. The *calibration bar* at lower right is 500 μm

Depth and location of responsive neurons

The responses of up to three neurons were isolated at each recording site: ~60% of the sites isolated one, ~32% two and ~8% three neurons. The first neural responses to whisker stimulation were commonly detected ~350 μm below the point of entry into cortex. The barrels in layer IV of rat S1 extend roughly from 450 to 800 μm in depth (Li et al. 2005). S2 cortex is slightly thicker than S1 and layer IV is less well defined. In the present study, 72% of the responsive neurons were encountered at depths between 450 and 650 μm in S1 and S2, respectively, placing them between deep layer III and mid layer IV. The remainder was in layer III.

A typical section through flattened cortex stained for cytochrome oxidase activity is shown in Fig. 2. The penetrations of the microelectrode arrays were clearly identifiable in most preparations as lines of four dark-rimmed punctures in the tissue. In our sample, S1 neurons responsive to whisker stimulation were located in the posterior part of the barrel field. Fifty-one cells could not be assigned to barrels or septa with certainty and were excluded from further analyses. We cannot rule out that a few neurons recorded from microelectrodes in the septa near the border of barrels were barrel cells. However, septum cells equally responded to the stimulation of several adjacent whiskers whereas barrel cells received their strongest input from one distinct principal whisker (Armstrong-James and Fox 1987; Brumberg et al. 1999), and we observed good correspondence between receptive field size and assigned location. Outside S1, responsive cells were scattered over a territory extending caudally and laterally to the row A barrels (Fig. 3; gray zone) within the boundaries in which Remple et al. (2003) mapped the face in S2 (their Fig. 3). The neurons in this zone possessed multi-whisker receptive fields that were ill defined to such extent that we could not distinguish more than one whisker representation.

Local responsiveness

Neural responsiveness decreased non-linearly with increasing stimulus frequency in S1 barrels, S1 septa and S2 conforming to the responsiveness of the sample as a whole. In spite of this similarity, however, we observed distinct differences among the local subpopulations.

Barrel neurons

Sixty-eight percent of the 111 responsive neurons in barrel columns responded to whisker stimulation with more than one discharge per ten stimuli. However, the percentage of neurons that responded exclusively to 1, 6 or 18 *apps*, decreased from 33 to 8 and 2%, respectively. In addition, 13% of the barrel neurons responded to 1 and 6 *apps* and 6% to 1, 6 and 18 *apps* (Table 1). Only one barrel neuron responded exclusively to 6 and 18 *apps*.

Septum neurons

Sixty-eight S1 neurons were located in septum columns. Seventy-seven percent of these neurons responded to

Table 1 Grouping of neural populations by response magnitude

	Total	Responsive	1	6	18	1 and 6	1, 6 and 18
All cells	479	285 (60%)	158 (33%)	31 (7%)	3 (0.6%)	68 (14%)	30 (6%)
S1 barrels	111	76 (69%)	37 (33%)	9 (8%)	2 (2%)	14 (13%)	7 (6%)
S1 septa	68	52 (77%)	25 (37%)	2 (3%)	0 (0%)	19 (28%)	6 (10%)
S2	249	120 (48%)	76 (31%)	6 (2%)	1 (0.4%)	23 (9%)	14 (6%)

Local prevalence of neurons that responded with at least one discharge per ten stimuli above spontaneous activity at 1, 6 and 18 *apps*. Only one neuron (a barrel cell) was found that exclusively responded to 6 and 18 *apps* and hence this combination is omitted. The percentages of the total are parenthesized

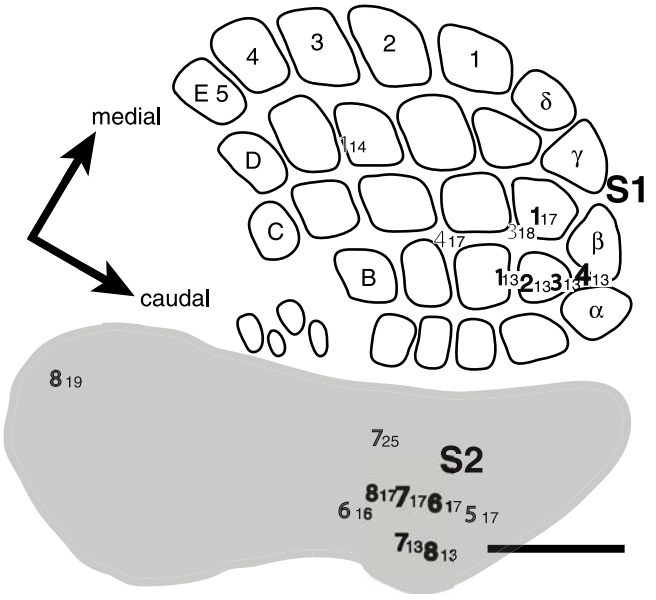

Fig. 3 Location of *full responders*. Electrode penetrations were traced on sections through flattened cortex stained for cytochrome oxidase (Fig. 2). The penetration numbers on the map mark the recording sites of *full responders* in respect to the barrels (straddlers, rows and arcs are *labeled*). The *boldness of the numbers* indicates how many *full responders* were isolated at that location (*thin* $n=1$, *medium* $n=2$, *thick* $n=3$). The *subscripts* specify the rat. The *gray zone* delineates the territory responsive to whisker stimulation outside S1. Except one cell, *full responders* in this zone were concentrated where the mystacial whiskers are represented in rodent S2. The *calibration bar* at lower right is 1,000 μm

whisker stimulation above threshold. The percentage of neurons responding exclusively to the low, middle and high stimulus frequency declined more precipitously than in the barrels, i.e., from 25 to 2 to 0%. However, more neurons in the septa responded to a wide range of stimulus frequencies than in the barrels, i.e., an additional 28% responded to 1 and 6 *apps* and another 10% responded to 1, 6 and 18 *apps* (Table 1).

S2 neurons

Two-hundred and forty-nine neurons responded to whisker stimulation in S2, 120 (48%) of which responded above threshold. This proportion is one third lower than that observed in S1 cortex. Thirty-one percent of the S2 neurons responded exclusively to 1 *apps*, 2% to 6 *apps* and 0.4% to 18 *apps*. An additional 9% responded to 1 and 6 *apps*, and 6% responded to 1, 6 and 18 *apps* comparable with the fractions observed in barrels (Table 1).

Global comparison of neural responsiveness

The majority of somatic sensory neurons responded above threshold to multi-whisker stimulation at low frequency. In S1, more barrel neurons responded to whisker stimulation than septum neurons except at 18 *apps* at which the proportions were equal. The approximate 3:2 ratio between barrel and septum neurons at stimulus frequencies up to 6 *apps* would apply to an estimated diameter of 500 μm for barrels and a width of 80 μm for septa; both realistic dimensions for posterior lateral barrel cortex. In proportion to sample size, however, more septum neurons were responsive above threshold than barrel neurons. This is also true for the comparison with S2 neurons.

The non-linear decline of neural responsiveness with increasing stimulus frequency left only one neuron in ten that discharged on average at least once every ten stimuli above spontaneous activity at the highest frequency, i.e., at 18 *apps*. Moreover, less than one neuron in 20 responded above this threshold only to 6 *apps* and one neuron in 100 only to 18 *apps*. Against this backdrop the neurons that were persistently and robustly activated above threshold across the entire range of stimulus frequencies are conspicuous. The stimulus-evoked discharge rates of these cells were statistically significantly greater than spontaneous activity in S1 barrels ($P=0.004$), S1 septa ($P=0.0001$) and S2 ($P=0.05$) in *z*-tests. We named the cells *"full responders"* and examine their responsiveness in detail below.

Full responders

Location

The full responders were isolated in roughly equal proportion in S1 (six barrel cells and six septum cells) and S2 (14 cells) in layer IV (mean depths: $S1_{septa}=480$ μm, $S1_{barrels}=580$ μm and $S2=510$ μm). One ($n=22$) or two ($n=4$) *full responders* were isolated at each recording site. The S1 cells were scattered across the three caudal arcs of rows B, C and D (Fig. 3). In S2, all cells except one were concentrated ~1,000 μm lateral and ~750 μm caudal to the A4 barrel (Fig. 3), i.e., where the mystacial whiskers have been mapped in rodent S2 in multiple studies (Woolsey and LeMessurier 1948; Woolsey and Van der Loos 1970; Carvell and Simons 1986; Krubitzer et al. 1986; Remple et al. 2003; Brett-Green et al. 2004).

Discharge characteristics

Figure 4 shows the action potentials and stimulus-evoked responses of typical *full responders* at the three locations. The action potentials of four of the six cells in barrels and septa returned to baseline within 750 μs qualifying them as fast-spiking neurons (Simons 1978; McCormick et al. 1985). In contrast, all but two S2 neurons produced action potentials longer than 750 μs, and the cells were classified regular-spiking. The S1 responses were tightly locked to stimulation at 6 and 18 *apps*, but their responsiveness adapted within ~20 s after the beginning of the stimulation epoch (Fig. 4; dot

raster displays). Neural responses in S2, in contrast, were not tightly locked to the stimulus and did not fall off as much with progressing stimulation as the responses in S1.

Figure 5 shows the raster plot data of Fig. 4 recast in peri-stimulus time histograms. Peaks of stimulus-locked discharge were distinct at 1 *apps*. The septum and the S2 neuron had additional peaks with fewer discharges, and their activity returned to spontaneous levels within 300 ms after stimulus onset. The additional peaks likely represent spindling activity initiated by whisker stimulation (Fox and Armstrong-James 1986). At 6 and 18 *apps*, peaks of periodic discharge were proportional to stimulus frequency, except in S2 at 18 *apps*. At 6 *apps*, the barrel neuron sustained discharge after the onset peaks whereas at 18 *apps* the septum cell showed distinct second peaks concomitant with stimulus offset. In comparison, the responses of the S2 neuron were less contoured, though a modulation of discharge commensurate with stimulus frequency and an earlier onset of response were noticeable at 6 *apps*.

Discharge rates

The discharge statistics of the *full responders* are listed in Table 2. The discharge rate denoted "υ" was calculated using:

$$\upsilon = (\text{number of discharges recorded during an epoch})/(\text{duration of the epoch [s]})$$

In Eq. 1, no constraints were imposed on the timing of the discharge during the epochs. Spontaneous activity was lowest in S1 barrels, slightly higher in S1 septa and about three times higher in S2. Conversely, whisker stimulation elevated the neural discharge rate on average threefold above spontaneous activity levels in S1 barrels, fivefold in S1 septa and only 1.5-fold in S2. Figure 6 depicts the average discharge rates above spontaneous activity (thick lines and symbols) across the spectrum of stimulus frequencies (f). Average neural discharge rates remained essentially unchanged in S1 barrels and S2 whereas S1 septum neurons showed a monotonic increase in mean discharge with increasing f (Fig. 6). The variability of the responses was highest among septum neurons with greatest standard deviations at 12 *apps*. The great margin was caused by three neurons with first derivative-bimodal, "hat-shaped" response functions peaking at 12 *apps*. Two barrel neurons also showed this type of response, but to a lesser degree. The most pronounced examples for these cells are shown in Fig. 6 (thin lines and symbols). In contrast, no hat-shaped response functions were found in S2. Though S2 neurons exhibited the greatest discharge rates, their dependence on stimulus frequency could not be established.

The number of discharges per stimulus denoted "#/stim" was determined using:

$$\#/\text{stim} = \upsilon/f[apps]. \quad (2)$$

In contrast to discharge rate, #/stim was greatest in S2, slightly lower in S1 septa and lowest in S1 barrels (Fig. 7) declining exponentially with increasing f. The decline was greatest in S2 ($\#/\text{stim}_{S2} = 2.7443 \times f^{-0.99}$), slightly less in barrels ($\#/\text{stim}_{S1\ \text{barrels}} = 1.2225 \times f^{-0.80}$) and smallest in septa ($\#/\text{stim}_{S1\ \text{septa}} = 1.4712 \times f^{-0.61}$) consistent with the monotonic increase in mean discharge rate at that location.

Latency

Neural discharge commonly peaked within 25 ms after stimulus onset. Across the range of stimulus frequencies, the grand median of modal latencies was shortest in S1 septa at 10 ms and equally long in S1 barrels and S2 at 25 ms (see Table 2). We observed dynamic relationships between the frequency of whisker stimulation and modal latency. Figure 8 shows the local cumulative distributions of first neural responses after each stimulus at 1, 6 and 18 *apps*. At the three locations, peaks of modal latency were most distinct at 1 *apps*. Latencies in barrels and septa peaked at 11 ms after stimulus onset whereas the modal latency was 52 ms in S2. Figure 9 illustrates the dynamics of latency across stimulus frequencies. Since numerous distributions were highly asymmetrical with long tails, medians and ranges are plotted. The medians suggest trends toward increasing latencies up to 9 and 15 *apps* in S1 septa and barrels, respectively, followed by a decrease to initial values. In contrast, at ≤ 3 *apps* median latency in S2 was five times greater than in S1 and diminished consistently with increasing stimulus frequency. It must be noted, however, that progressively more first responses occurred at longer latencies and the peaks of modal latency became less defined (Fig. 8) suggesting that neural responses in S2 were less tightly locked to the stimulus. In S1, in contrast, barrel and septum cells maintained pronounced peaks of modal latency (Fig. 8). These differences in response accuracy were examined further with analyses of autocorrelation.

Autocorrelations

The relationship between temporal accuracy of response and frequency of whisker stimulation is illustrated in Fig. 10. The autocorrelograms show the average coincident responses of the local subpopulations of *full responders* (Aertsen et al. 1989). No coincidences of neural responses were found at time zero. However, only the autocorrelograms of S2 neurons show a distinct notch (Fig. 10c). At 1 *apps*, the center peak was most prominent in S1 septum cells. Smaller peaks on each side of the main peak indicate minor coincident responses at ± 80 ms due to spindling (Fig. 5). In S1 barrels and S2, in contrast, coincident discharges were more dispersed and only small peaks were noticeable. At 3 *apps* (Fig. 10, insert), barrel neurons began to show distinct peaks of coincident responses to same- (near 0 s) and mixed-order stimuli (at ± 330 ms). Barrel as well as septum

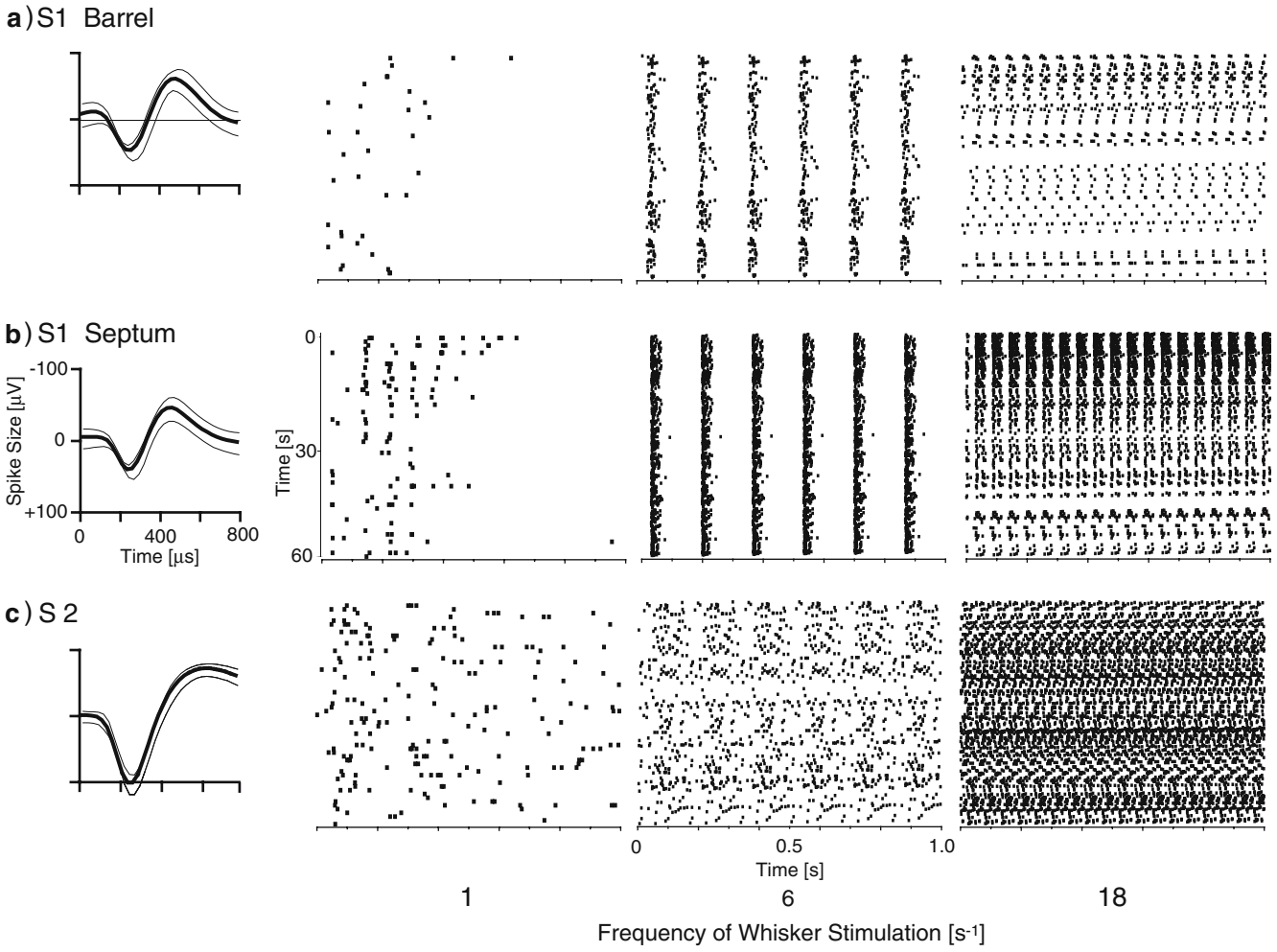

Fig. 4 Action potentials and peri-stimulus raster plots of *full responders*. Each row shows results from a typical cell in S1 barrels (**a**), S1 septa (**b**) and S2 (**c**), respectively. The mean waveforms of the action potentials (*thick line*) ± 1SD (*thin lines*) of all discharges recorded with a set of stimuli are shown in the *left column*. The action potentials of S1 cells usually returned to baseline within 750 µs and these neurons thus qualify as fast spiking. The discharge of the S2 neuron, in contrast, exceeded this limit and qualified as regular spiking. The discharges of the cells during 60-s episodes of whisker stimulation with 1, 6 and 18 *apps* are shown in the *peri-stimulus dot raster plots* on the *right*. The data was segmented into 1-s windows with 2-ms binning

neurons produced the greatest peaks at 6 *apps*, i.e., the greatest number of coincidences occurred near the dominant whisk frequency (Carvell and Simons 1990; Fanselow and Nicolelis 1999; Gao et al. 2001). Although the peaks of barrel neurons were smaller than those of septum neurons, the FWHM was at 18 ms significantly narrower than that of septum neurons at 29 ms ($P = 0.01$; *Wilcoxon* test) approaching the passive membrane time constants for postsynaptic potentials of cortical neurons (König et al. 1996). Hence, barrel neurons may constitute better co-incidence detectors than septum neurons.

Remarkably, in barrels and septa alike the subordinate peaks were taller than the center peak. These peaks represent coincident responses to mixed-order stimuli, i.e., responses to the first stimulus coincided with those to the second stimulus, responses to the second stimulus with those to the third and so forth. The increase in size of the subordinate peaks with distance from the center peak indicates that the neural responses to mixed-order stimuli became more numerous with decreasing rank order than the responses to same-order stimuli. This finding suggests that the S1 neurons frequently responded to stimuli with delays that were precisely matched to the inter-stimulus interval. The autocorrelograms in barrels deteriorated ≥15 *apps* whereas in septa peaks of coincident response commensurate with stimulus frequency were still distinct at 18 *apps*. Septum neurons seem, therefore, better suited to resolve differences in stimulus frequency over a broader range than barrel neurons. In contrast to S1, the response behavior in S2 remained distinctly unaffected by stimulus frequency. No peaks of autocorrelation were observed comparable to those of S1. At 6 stimuli/s, only small undulations could be detected on a broad hump of dispersed, randomly coincident discharge.

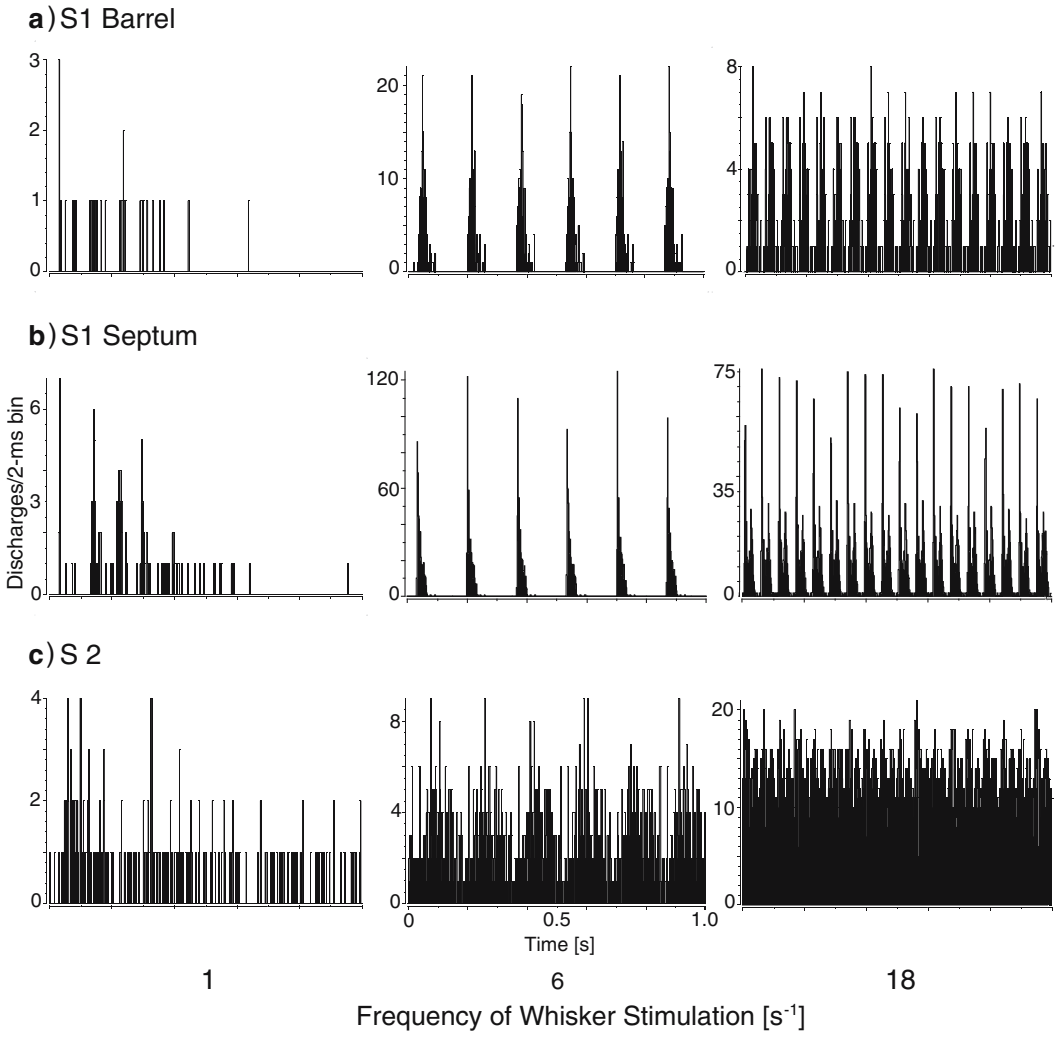

Fig. 5 Peri-stimulus time histograms of *full responders*. Responses of the cells in Fig. 4 accumulated over 1 min of stimulation and plotted in 1-s windows (bin width = 2 ms). The histograms demonstrate the temporal accuracy of neural responses to whisker stimulation at 1, 6 and 18 *apps*. In S1 barrel (**a**) and S1 septum (**b**) cells, responses were concentrated in narrow peaks commensurate with the frequency of whisker stimulation at 6 and 18 *apps*. In contrast, the discharge in S2 (**c**) was more dispersed. Distinct peaks formed only at 1 and 6 *apps*. At 1 *apps*, the septum cell (**b**) and the S2 cell (**c**) had sustained responses of lower magnitude up to 400 ms after stimulus onset. Note the varied response magnitude expressed by the differences in scaling

Stimulus–response correlations

The autocorrelation analyses above suggest that the temporal accuracy of responsiveness deteriorated with increasing frequencies of whisker stimulation more in barrels than in septa. This degradation may have been the result of stimulus frequency-dependent shifts in synchrony of neural responses, and these shifts may also account for the low temporal acuity of S2 cells. In order to test this hypothesis, we determined the coefficients of correlation between the time course of discharge of each neuron and the time course of the air puffs at the corresponding frequency of whisker stimulation. This method was chosen over other methods used with

Table 2 Discharge types, rates and latency of response of *full responders*

	Number of cells	Fast-/ regular-spiking	Bursts per cell[2]	Spontaneous discharge rate (s^{-1})[a]	Stimulus-evoked discharge rate υ (s^{-1})[a]	Discharges per stimulus[a]	Latency (ms)[b]
Barrels	6	4/2	28	0.55 ± 0.70	1.83 ± 0.27	0.42 ± 0.49	25
Septa	6	4/2	34	0.67 ± 0.90	3.25 ± 1.06	0.56 ± 0.40	11
S2	14	2/12	50	1.83 ± 1.71	2.75 ± 0.30	0.65 ± 0.77	25

Averages across all frequencies of whisker stimulation (means and standard deviations[a] or medians[b])

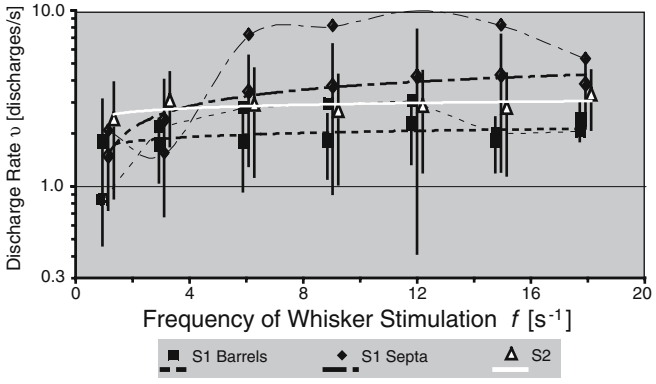

Fig. 6 Neural discharge rate as function of stimulus frequency. Mean discharge rates (υ) ± 1SD and logarithmic trend lines of best fit are plotted against the frequency of whisker stimulation (f) for *full responders* in S1 barrels ($n=6$, *squares*, *thick dashed line*), S1 septa ($n=6$, *diamonds*, *thick interrupted line*) and S2 ($n=14$, *triangles*, *solid line*). The data are plotted staggered on the abscissa to improve separability. Average spontaneous discharge was subtracted. The mean discharge rate grew persistently with f only in the septa though three cells expressed first-derivative bimodal, "hat-shaped" stimulus/response functions. Also two barrel cells exhibited such response functions. The *small symbols* and *thin lines* represent the extreme cases at each location. This type of response was not observed in S2

sinusoidal stimuli (Fee et al. 1997; Garabedian et al. 2003; Khatri et al. 2004), because it is unconstrained by the shape of the stimulus and provides a simple measurement for the tightness of the temporal association between stimulus and response. At 1 *apps*, the correlation coefficients at the three cortical locations clustered around $r=0.3$ (Fig. 11). With increasing stimulus frequency, however, two distinct groups of positive (>0.2) and negative (<-0.2) coefficients evolved that were

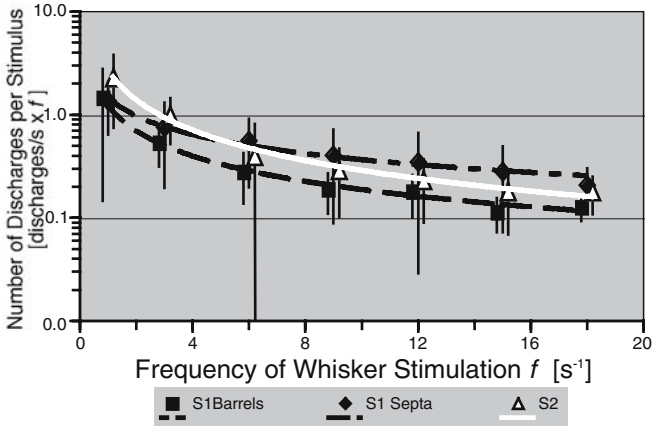

Fig. 7 Neural responsiveness normalized by frequency of whisker stimulation. Mean neural discharges per stimulus ± 1SD are plotted as a function of stimulus frequency for each subpopulation of neurons. *Symbols* and *lines* identify cortical location as in Fig. 6. Power functions were the best fits for the trends in each subpopulation. At the three locations, f-normalized discharge declined exponentially reaching asymptotes above 9 *apps*. S2 neurons featured the highest responsiveness at 1 *apps* and the steepest decline

furthest apart at 18 *apps* (Fig. 11a) suggesting that the population of *full responders* in somatic sensory cortex gravitated toward a bi-stable steady state. Since the air puffs deflected the whiskers rostro-caudally, neural discharge with positive correlation was synchronous with the deflection of whiskers in the direction of retraction and negative correlation was synchronous with the direction of protraction. The paucity of correlation coefficients in the range of $-0.2 \le r \le 0.2$ indicates that the *full responders* discharged most vigorously when the whiskers accelerated in motion and the synchrony of discharge with whisker movement strengthened with increasing stimulus frequency. This synchrony was not stationary across frequencies. Neural responses occasionally *flipped* into the opposite state from one stimulus frequency to the next while the strength of the correlation was preserved or improved (the thin lines in Fig. 11a show typical examples for each cortical location).

The absolute magnitude of the correlation coefficients measures the strength of the temporal association between neural discharge and whisker motion (Fig. 11b). It therefore may serve as indicator of the sign-independent synchronization of stimulus and neural response. The median across stimulus frequencies was greatest in S1 septa ($|r|=0.45$), and about equal in S1 barrels ($|r|=0.29$) and S2 ($|r|=0.30$). In the septa, this synchrony improved steadily with increasing frequency of whisker stimulation reaching the highest median among the three cortical locations at 18 *apps*. In contrast, in the barrels the synchrony remained unaltered up to 12 *apps*, above which it increased threefold whereas only inconsistent change was observed in S2. The strong improvement in barrel cells supports our hypothesis that the deterioration of temporal acuity at 18 *apps* apparent in Fig. 10 is most likely the result of shifts from synchronous to anti-synchronous responsiveness of individual cells rather than the deterioration in the temporal organization of their responses.

Discussion

Major findings

About 60% of the neurons responsive to whisker stimulation discharged above spontaneous activity more than once per ten stimuli. The vast majority surmounted this threshold only at frequencies below 6 *apps*. Neurons rarely responded above threshold exclusively at the middle or the high stimulus frequencies. In striking contrast, 26 neurons that were equally distributed in S1 and S2 responded above threshold across the full range of stimulus frequencies employed. We presume these *full responders* would be best suited to play a crucial role in frequency discrimination because they appear to be optimally poised to support the differentiation of stimulus frequencies that rats are commonly exposed to when they explore their environment with their

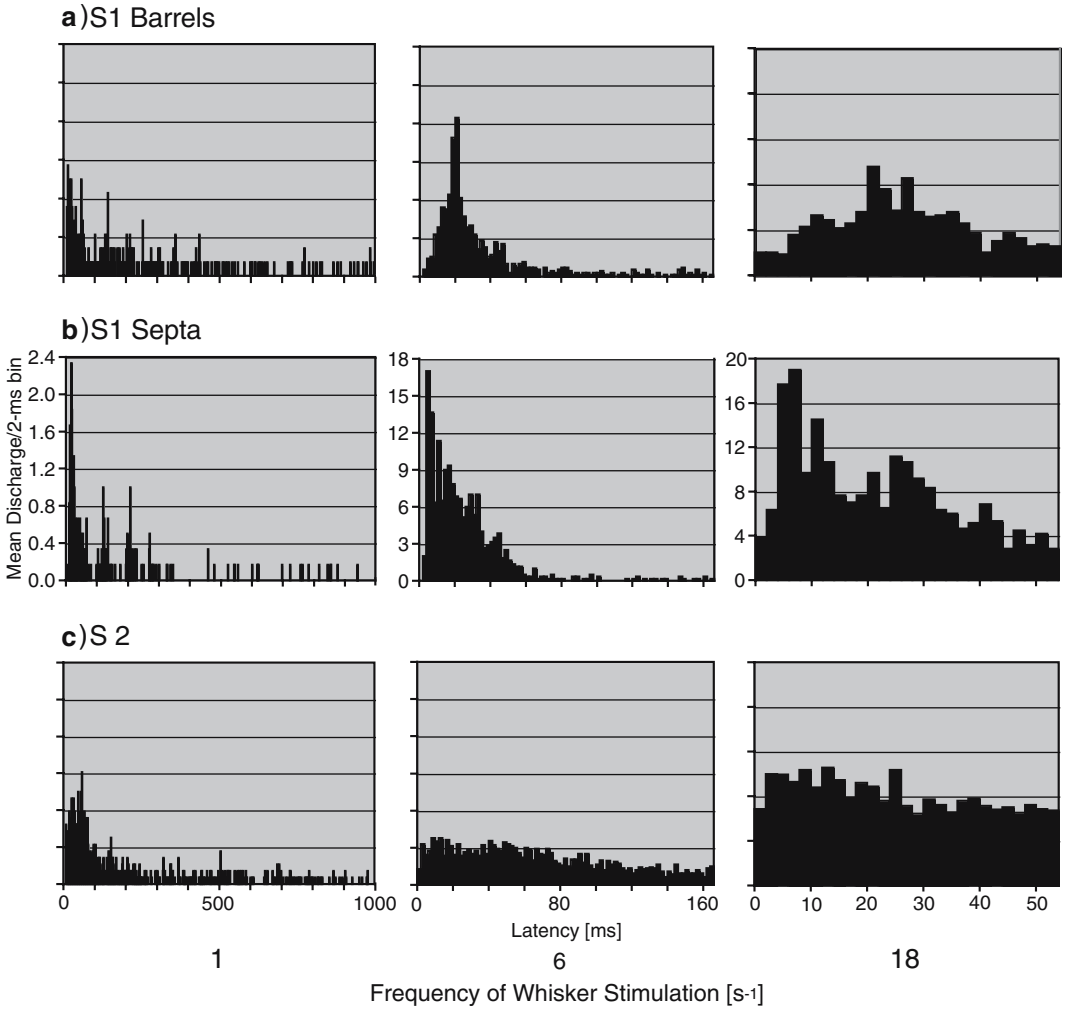

Fig. 8 Latency of response. The latency histograms display the cumulative first responses after stimulus onset (corrected for air puff delay and a 3-ms refractory period) from the subpopulations of *full responders* in S1 barrels (**a**), S1 septa (**b**) and S2 (**c**) at 1, 6 and 18 *apps*. In each column, the abscissa is scaled to the duration of the inter-stimulus interval and the ordinate is scaled to the highest peak. The stable distributions in S1 (**a** and **b**) indicate that latencies remained focused across stimulus frequencies. Barrel neurons showed the smallest spread toward longer latencies. In S2, in contrast, a dominant latency appears to be salient only at 1 *apps* while the neurons discharged with little temporal specificity at 6 and 18 *apps* (**c**)

whiskers. *Full responders* exhibited locally distinct peculiarities in rate and temporal accuracy of discharge. Six differences were striking:

1. Most *full responders* in S1 were fast spiking whereas the majority in S2 was regular spiking.
2. Spontaneous neural activity in S2 was twice that of S1 and the cells discharged in bursts more frequently than in S1.
3. The discharge rates in S1 barrels and S2 remained unchanged across the range of stimulus frequencies. In contrast, S1 septum neurons increased their discharge rate progressively with increasing stimulus frequency.
4. Neural responses adapted progressively with increasing frequency of whisker stimulation. The discharge per stimulus rapidly declined at the three locations examined and the values hardly differed ≥9 *apps*. The highest magnitude and the steepest decline were observed in S2.
5. Modal latency of response averaged across all stimulus frequencies was shortest in S1 septa and about equal in S1 barrels and S2. However, at low frequencies latencies in S2 were greater than in S1 whereas the converse was true at high frequencies.
6. The temporal accuracy and synchrony with which neural discharge followed whisker stimulation were greater in S1 than in S2 across all stimulus frequencies.

These differences in responsiveness suggest that the cells examined in S1 barrels, S1 septa and S2 may play functionally distinct roles in the processing of tactile input. Moreover, S2 may receive input from different sources than S1. The implications of our observations and methodological aspects affecting them are discussed in detail below.

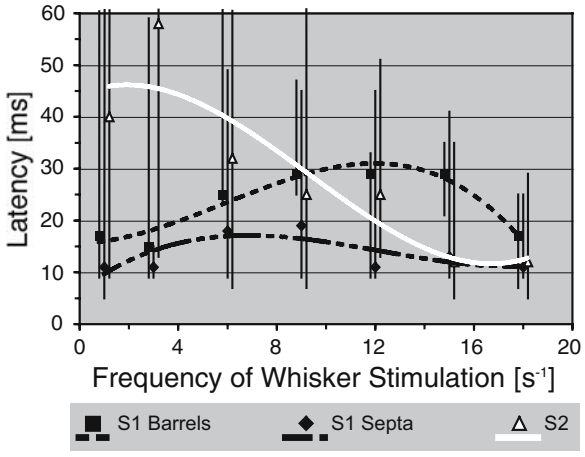

Fig. 9 Modal latency of the population response as a function of frequency of whisker stimulation. Medians and ranges of modal latencies are plotted against stimulus frequency. *Symbols* and *lines* identify cortical location as in Fig. 6. Third degree polynomial functions were the best fits for the trends in each subpopulation. In S1, modal latency roughly doubled with increasing stimulus frequency up to 9 and 15 *apps* for septa and barrels, respectively. At higher stimulus frequencies, latencies shortened to the values found at 1 *apps*. The S2 cells, in contrast, had modal latencies at stimulus frequencies ≤ 3 *apps* that were on average four to five times greater than in S1, but appeared to shorten to comparable levels with increasing stimulus frequency

Methodological considerations

In the present study, we consider neurons that responded above their spontaneous rate on average at least once per ten stimuli at frequencies of whisker stimulation between 1 and 18/s. These conditions were selective for cells that increased discharge without imposing any restrictions on the timing of the discharge during the 1-min epoch of recording. Conversely, cells were excluded that re-arranged their discharges in respect to stimulus onset without changing their average discharge rates. The thresholding of responsiveness isolated a set of neurons that responded with equal robustness across stimulus frequencies and recordings distilling a comparable sample with distinct physiological properties in spite of the variability in numbers and positions of the stimulated whiskers.

The stimulus

The air puffs produced stable, reproducible deflections of multiple whiskers including the principal whisker for each recording site. Neurons in barrel cortex respond to the transients of pulsatile whisker deflection (Khatri et al. 2004). The pressure of the air puffs was set to provide transients driving neural responses effectively even when the baseline pressure increased at frequencies ≥9 *apps* transitioning the stimuli from fully recursive motion to ramp-and-hold deflections. A diminishing baseline-to-peak pressure could account for dampened neural discharge. However, in the present study the observed reductions in neural discharge per stimulus reached asymptotes at frequencies below 9 *apps*. At these frequencies, the shape of the pulse was not altered and baseline-to-peak pressure was stable at 13 ± 1 kPa. Moreover, very few neurons responded only to high-frequency whisker stimulation. Hence, we conclude that the changes in neural discharge rate observed in the present study were the result of the differences in the frequency of whisker stimulation.

The number of stimulated whiskers may be crucial to the observed changes in neural discharge rate. Tonic discharge increases with increasing stimulus frequency when a single whisker is stimulated with 3–10 stimuli/s (Garabedian et al. 2003). The stimulation of multiple adjacent whiskers facilitates neural responsiveness when the whiskers are stimulated within ~5 ms (Ghazanfar and Nicolelis 1997; Shimegi et al. 1999, 2000). However, only a minority of layer IV neurons showed this synergy. Shimegi et al. (1999, 2000) demonstrated facilitation for 42 of 114 cells analyzed; only five cells were in layer IV and those were in septa. In contrast, the response of most layer IV neurons to the stimulation of the principal whisker appears to be diminished by the concomitant stimulation of surround whiskers yielding fewer neural responses than the stimulation of individual whiskers (Moore et al. 1999; Mirabella et al. 2001). The diminution can be attributed in part to intracortical inhibition mediated by GABAergic non-spiny stellate cells in layer IV (Armstrong-James et al. 1994). The receptive fields of neurons in the S1 barrel cortex are composed of an excitatory center driven by inputs from the principal whisker, an excitatory surround and an inhibitory surround (Simons 1978; Armstrong-James and Fox 1987). Stimulation of surrounding whiskers up to inter-stimulus intervals of ~30 ms suppresses the input from the principal whisker (Simons 1983; Derdikman et al. 2003). In line with the findings of Mirabella et al. (2001) and Moore et al. (1999), our observations suggest that during the simultaneous stimulation of principal and surround whiskers surround inhibition takes precedence over surround excitation.

Anesthesia

We used urethane as anesthetic because this drug provides stable recordings over a long period of time (Armstrong-James and George 1988), produces receptive fields only slightly larger than in unanesthetized preparations (Simons et al. 1992) and does not affect neural responsiveness to passive whisker stimulation (Castro-Alamancos 2004; Krupa et al. 2004). The *full responders* constituted only a small fraction (6%) of the somatic sensory neurons responsive to whisker stimulation. The cells were found in seven animals. Most were isolated in two rats. The low prevalence of the *full responders* as well as their derivation from a small number of animals may be related to the depth of anesthesia. With deeper anesthesia, neural responsiveness,

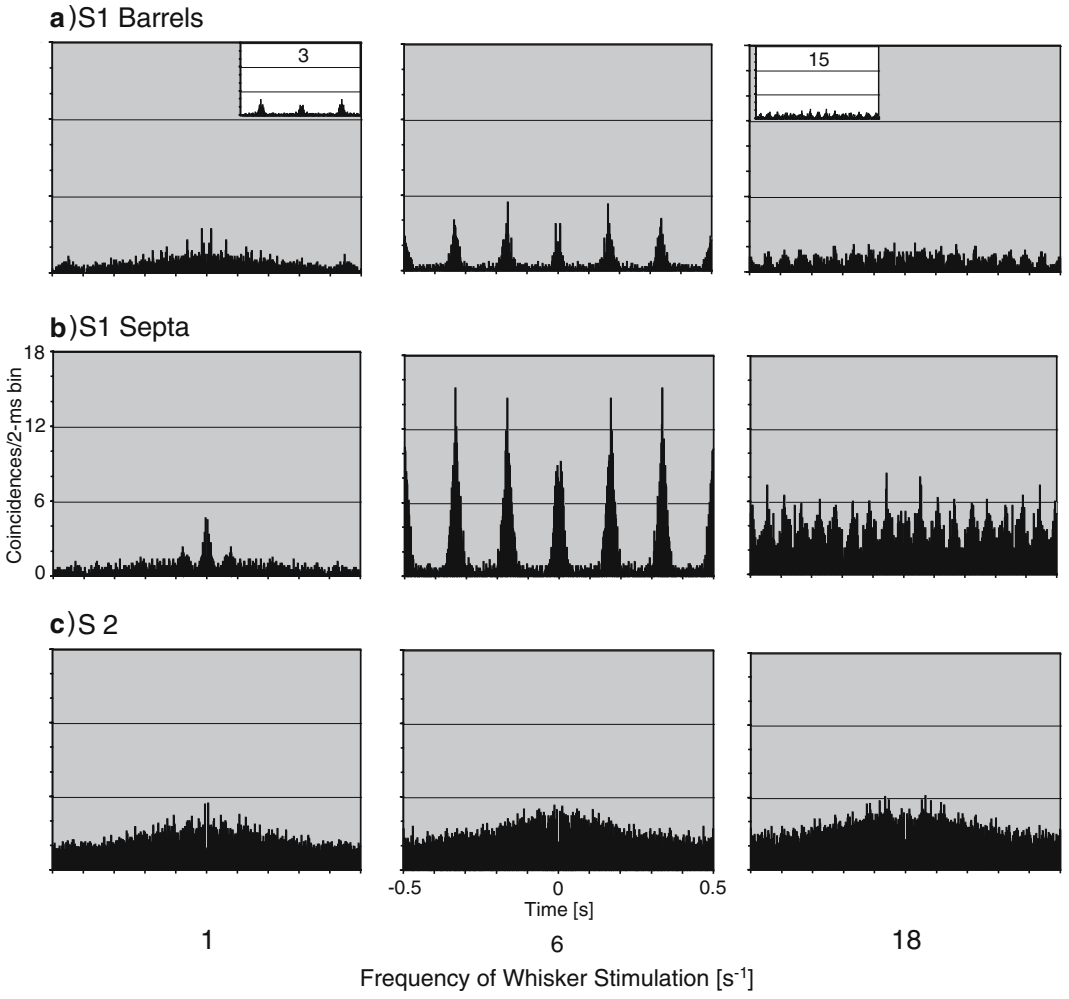

Fig. 10 Autocorrelation of neural responses. The average autocorrelograms of *full responders* in S1 barrels (**a**), S1 septa (**b**) and S2 (**c**) are shown at 1, 6 and 18 *apps*. At center peak, neural responses to the same-order stimuli coincide. Septum cells exhibit distinct center peaks across the entire range of stimulus frequencies. Subordinate peaks are prominent at 6 and 18 *apps* (**b**). Autocorrelograms of barrel neurons are similar between 3 and 15 *apps* (**a**, inserts). Owing to stimulus-locked spindling at 1 *apps*, the septum cells expressed additional smaller peaks at about 80 ms on either side of the center peak (**b**). At 6 *apps*, the subordinate peaks in barrels (**a**) and septa (**b**) were greater than the center peak indicating frequent delayed coincident discharge. In contrast, no distinct peaks and only faint modulation of coincident responsiveness are noticeable in S2 (**c**)

spontaneous activity and the size of neural receptive fields diminish (Friedberg et al. 1999; Erchova et al. 2002). While less than one third of the neurons responded below threshold in barrels and septa, more than half did so in S2. Similar fractions of so called ''unresponsive'' neurons have been reported by others using anesthetized preparations (Mountcastle 1957; Levitt and Levitt 1968). Dykes and Lamour (1988) even report that 75% of 534 neurons in rat S1 were unresponsive to stimulation under urethane or halothane anesthesia. In contrast, in awake rabbits the fraction of unresponsive neurons was smaller than that of the present study, i.e., 22% of 396 neurons recorded in S1 (Swadlow 1989) and 31% of 306 neurons in S2 were unresponsive (Swadlow 1991). Consistent with these findings, S1 neurons exhibited a greater tonic discharge in awake, actively discriminating rats than with passive whisker stimulation or under anesthesia (Krupa et al. 2004) and no adaptation of responsiveness to sensory stimulation was observed (Castro-Alamancos 2004). Taking these findings together, *full responders* may gain prevalence in un-drugged animals and this hypothesis is under investigation in our laboratory.

Conceptual considerations

Rate code

In S1 barrels and S2, average neural discharge rates remained essentially unchanged across the range of stimulus frequencies employed. In both locations, therefore, the discharge rate of *full responders* is not sufficient to encode stimulus frequency. However, the

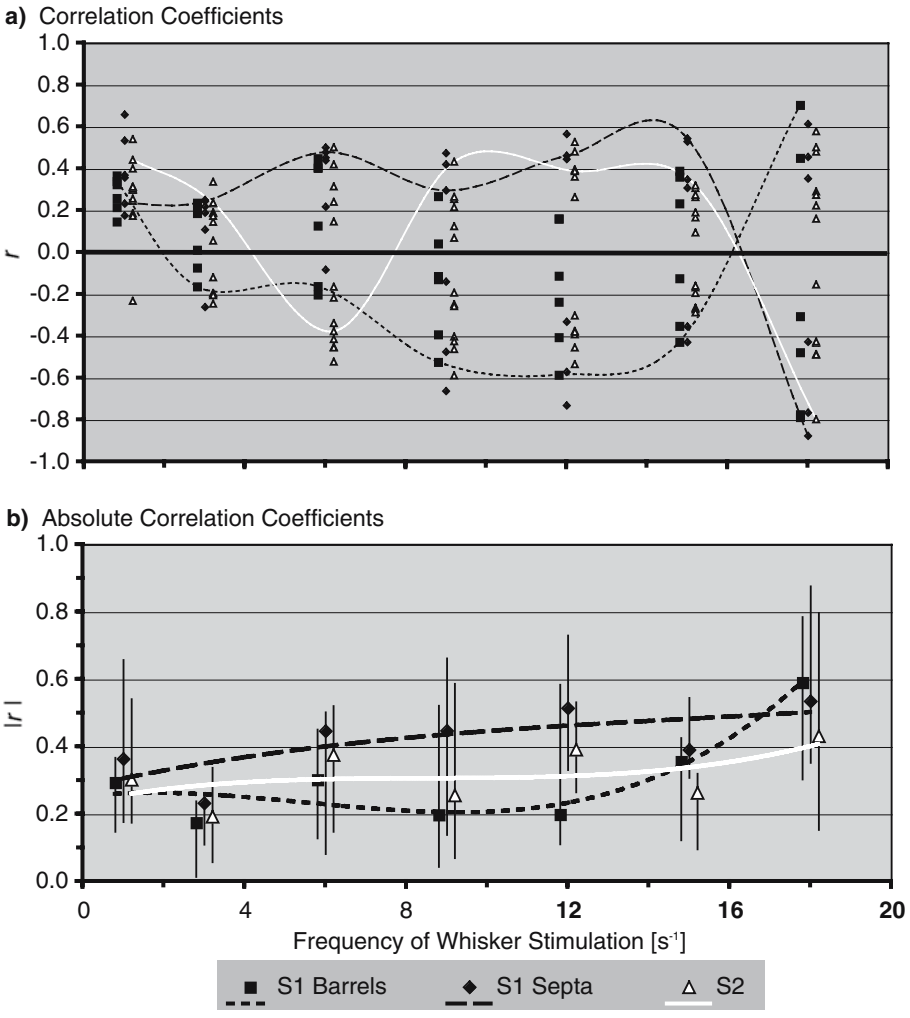

Fig. 11 Correlation of neural discharge with whisker stimulation. Correlation coefficients for each cell (**a**) and absolute median correlation coefficients, ranges and third degree polynomial fits for each group (**b**) are plotted as a function of stimulus frequency. *Symbols* and *lines* identify cortical location as in Fig. 6. Frequencies likely to generate ramp-and-hold whisker deflection ("flutter") are printed in *bold face*. The coefficients express the tightness of the temporal association between stimulus and response. With increasing stimulus frequency correlation coefficients diverged into positive and negative quadrants (**a**). The dichotomy was produced by inversions in sign of the coefficients of individual neurons (lines in **a**). However, the absolute strength of correlation increased with increasing frequency of whisker stimulation, particularly in the barrels (**b**)

discharge per stimulus at the three locations examined declined exponentially with increasing frequency of whisker stimulation consistent with the findings of others in barrel cortex (Simons 1978; Ahissar et al. 1997, 2001; Fanselow and Nicolelis 1999; Chung et al. 2002; Kleinfeld et al. 2002; Garabedian et al. 2003; Castro-Alamancos 2004; Khatri et al. 2004). The decline in response magnitude may be the result of short-term synaptic depression at thalamocortical afferents (Castro-Alamancos and Oldford 2002; Chung et al. 2002; Khatri et al. 2004) paired with intracortical inhibition.

In the present study, the determination of neural discharge/stimulus was not limited to a window in time after stimulus onset. Rather, the mean above spontaneous discharge was averaged over the entire minute of recording. Hence the diminution of responsiveness was not attributable to a dispersal of the discharge, but constituted an actual decrease in neural spiking activity. This decrease was greatest in the cortical area with the highest rate of spontaneous activity, i.e., S2, and low frequencies of whisker stimulation could be encoded in a negative rate code provided the neurons obtained precise information about the timing of the stimuli. Ahissar et al. (1997) suggest that stimuli below 12/s may be timed with sufficient precision by thalamo-cortico-thalamic feedback loops that force intrinsic neural oscillators to lock in phase with tactile input. Hence, somatic sensory cortex may possibly act as a low-pass filter utilizing an inverse proportional code and, if so, S2 provides the narrowest filtering.

Since the observed sensory adaptation entailed a non-linear decrease in the discharge/stimulus as well as in the number of responsive neurons, both effects together seem necessary to produce first derivative-bimodal stimulus/response functions observed in numerous functional imaging studies to peak between 3 and 6 stimuli/s (Moskalenko et al. 1996; Vogel and Kuschinski 1996; Detre et al. 1998; Ngai et al. 1999; Silva et al. 1999; Hewson-Stoate et al. 2005; Melzer and Ebner 2004; Ureshi et al. 2004). The prominence of such stimulus/response functions in the imaging literature emphasizes the crucial role that the relationship between neural discharge rate and the frequency of sensory stimulation plays in the population response of cortical neurons. The *full responders* constitute examples for neurons that could drive local blood flow dependent on their broadband responses.

Neurons in the septa constitute an exception to the conclusions above. These neurons had the lowest spontaneous activity and were the only candidates in rat somatic sensory cortex that were able to increase average discharge rate continuously with increasing frequency of whisker stimulation. Hence, these cells may provide a substrate for a positive rate code fundamental to information processing in an integrate-and-fire mode (for review see König et al. 1996).

Latency

Latency of neural responses to whisker stimulation was measured as the period of time between the onset of the air puff and the peak of first neural response accumulated over the entire minute of recording. The observed latencies of response in barrels (25 ms) and septa (11 ms) are substantially different from those usually reported. Ito (1985) determined 9.5 ms for neurons in barrel cortex. Armstrong-James and Fox (1987) report that most barrel neurons respond with modal latencies of less than 10 ms to the deflection of their principal whisker. Stimulation of one (Kleinfeld et al. 2002) or more (Ahissar et al. 2001) whiskers with air puffs gave similar latencies only when the response to the first stimulus in a train was measured. In contrast, the cumulative modal latencies we observed are consistent with the latencies Brecht and Sakmann (2002) determined with intracellular recordings. These authors report that the peak response latencies to the deflection of the principal whisker were significantly shorter in barrels (15.0 ms) than in septa (22.3 ms). However, when surround whiskers were stimulated, septum neurons responded at shorter latency (17.8 ms) than barrel neurons (23.5 ms). In the present study, principal and surround whiskers were stimulated nearly simultaneously, and this combination may have resulted in the shorter latency of response in the septum neurons. Barrel neurons receive input via the lemniscal pathway, and neurons in septa and in upper layer V beneath the barrels receive input via intracortical and paralemniscal pathways (Koralek et al. 1988; Chmielowska et al. 1989; Diamond et al. 1992; Lu and Lin 1993; Kim and Ebner 1999; Pierret et al. 2000). The observed antecedence of septa over barrels provides further evidence that rat S1 cortex receives thalamocortical input from separate ascending pathways.

Consistent with findings in pentobarbital-anesthetized (Garabedian et al. 2003) and alert, whisking rats (Fanselow and Nicolelis 1999), latencies of septum and barrel neurons increased with increasing frequency of whisker stimulation up to 9 and 15 *apps*, respectively. In accord, Whitsel et al. (2003) observed a frequency-related increase in latency of neural response in macaque S1 cortex during vibrotactile stimulation of the glabrous skin. Ahissar et al. (2000, 2001) attributed the greatest latency increases in barrel cortex to neurons in upper layer V receiving paralemniscal input from the posterior thalamic nucleus, though their data shows a distinct increase also in barrel neurons at the highest frequency of stimulation used in that study (11 *apps* in Fig. 6; Ahissar et al. 2001). These authors observed that the neural discharge per stimulus decreased with increasing latency, because the time available for discharge shortened. This mechanism may possibly apply to the *full responder* neurons in S1.

Since S2 receives thalamic input via a non-lemniscal route (Carvell and Simons 1987; Spreafico et al. 1987; Koralek et al. 1988; Kim and Ebner 1999; Pierret et al. 2000) in addition to S1 (Carvell and Simons 1987; Fabri and Burton 1991), S2 may constitute the cortical termination of a parallel ascending somatic sensory pathway (Zhang et al. 2001). In the present study the median latency in S2 was five times greater than in S1 at low stimulus frequencies suggesting that S2 is activated by prominent corticocortical input, most likely from S1.

Discharge timing

In primates, the tactile perception of the roughness of gratings appears substantially influenced by the temporal frequency of the gratings and this frequency is tightly associated with the phase-locked discharge of primary afferents as well as thalamic and cortical neurons (Cascio and Sathian 2001). Consistent with these findings, the *full responders* responded to whisker stimulation with frequency-related, highly structured temporal patterns of periodic discharge. Autocorrelation of neural responses showed that barrel neurons discharged with the greatest temporal accuracy at frequencies pertinent to exploration (3–15 *apps*). Septum neurons responded less accurately, but their responsiveness remained stable across the entire spectrum of frequencies examined (1–18 *apps*). In contrast, neural responsiveness in S2 showed little temporal accuracy.

The synchrony of neural discharge with whisker stimulation constitutes a major factor affecting the temporal accuracy of the population response. We examined this relationship using coefficients of correlation between the time courses of neural response and the air puffs. Although the response of many cells appeared to be positively correlated with stimulation, a greater number discharged in progressively negative correlation with increasing stimulus frequency resulting in the greatest variation of correlation coefficients at the highest frequency. The high negative correlation coefficients imply that the neurons discharged locked to stimulation, though the discharges lagged behind the onset of the air puffs by half an inter-stimulus interval (~28 ms). Consistent with our observations, Khatri et al. (2004) observed that the steady-state responses of neurons in barrel cortex were predominantly anti-phasic at high stimulus frequencies and similar shifts in phase were observed in macaque S1 with vibrotactile stimulation of the glabrous skin (Whitsel et al. 2003).

S2 vs S1

Our findings are remarkably similar to those in primates in that neurons responded to whisker stimulation in discharges that were locked to the stimuli sufficiently tightly across frequencies to support temporal encoding in S1 (Sinclair and Burton 1991; Hernández et al. 2000) whereas this accuracy was lacking in S2 (Pruett et al. 2000; Salinas et al. 2000). S2 neurons showed the least coherent changes in synchrony of discharge, and a loss in temporal accuracy of the population response was not attributable to shifts in phase as in S1. The phase-locking between stimulus and response may improve, however, when rats are awake and move their whiskers purposefully in a tactile discrimination task. Compared to passive stimulation, active discrimination appears to synchronize neural discharge in rat S1 (Ganguly and Kleinfeld 2004) and in both S1 and S2 of macaque monkeys (Salinas et al. 2000). Most intriguingly, however, we observed cortical area-specific changes in neural discharge rate and discharge per stimulus with increasing stimulus frequency providing evidence for the possibility of a rate code (Hernández et al. 2000; Salinas et al. 2000). Notably, S1 septum *full responders* increased their discharge rate proportionately with increasing stimulus frequency. An analog to septum cells has not been described in primates.

The action potentials of the *full responders* in S2 were distinctly different from those in S1. Using the classification of McCormick et al. (1985), the majority of S1 *full responders* were fast-spiking whereas S2 *full responders* were regular-spiking and bursting. These authors associated the fast-spiking neurons with aspiny or non-spiny GABAergic stellate cells presumed to be inhibitory interneurons, whereas regular-spiking neurons are presumably excitatory spiny pyramidal or stellate cells. Bursting cells were most frequent in layer IV (McCormick et al. 1985). The fast-spiking cells in S1 barrel cortex may provide the inhibition to the neurons that cease responding with increasing frequency of whisker stimulation. In contrast, consistent with the prominence of regular-spiking cells S2 contains fewer inhibitory cells in layer IV than barrel cortex. This difference may explain the greater levels of spontaneous activity, the higher stimulus-related discharge, the bursting, and the larger receptive fields in S2 than in S1 observed in the present and other studies (Welker and Sinha 1972; Burton et al. 1982; Carvell and Simons 1986; Swadlow 1991; Remple et al. 2003; Brett-Green et al. 2004).

Full responders in S2 did not appear to use either precise timing of discharge or discharge rate to encode stimulus frequency. However, compared to the S1 cells, their discharges per stimulus declined most profoundly with increasing stimulus frequency. Hence, modulation of discharge gated by stimulation appears to be the most likely code for the frequency of whisker stimulation in S2. In combination with the large receptive fields, S2 may be most suitable to encode slow aspects of whisker touch, such as interactions between whiskers on both sides of the face (Carvell and Simons 1986), and may provide feed-forward input facilitating neural responses in S1 and motor cortex. Perhaps, when paired with inputs from other modalities a synergistic response may arise (Wallace et al. 2004) that alerts the animal to an obstacle in a specific tactile hemi-field. Several studies have begun to examine bilateral information processing in rat somatic sensory cortex (Pidoux and Verley 1979; Dörfl et al. 1988; Champney et al. 2001; Krupa et al. 2001; Shuler et al. 2001), but the functional interactions between S2 with S1 remain an open question.

Acknowledgements We are indebted to Robert N.V. Sachdev for his instrumental role in the early phases of this study and for his many discussions on the subject. Michael Armstrong-James is thanked for his cogent advice. This research was supported by Public Health Service grants to Ford Ebner (NS-25907), the J.-F. Kennedy Center for Research in Human Development (HD-15052) and the Vanderbilt Vision Research Center (EY-08126).

References

Aertsen AMH, Gerstein GL, Habib MK, Palm G (1989) Dynamics of neuronal firing correlation: modulation of "effective connectivity". J Neurophysiol 61:900–917

Ahissar E, Kleinfeld D (2003) Closed-loop neuronal computations: focus on vibrissa somatosensation in rat. Cereb Cortex 13:53–62

Ahissar E, Haidarliu S, Zacksenshouse M (1997) Decoding temporally encoded sensory input by cortical oscillations and thalamic phase comparators. Proc Natl Acad Sci USA 94:11633–11638

Ahissar E, Sosnik R, Haidarliu S (2000) Transformation from temporal to rate coding in a somatosensory thalamocortical pathway. Nature 406:302–306

Ahissar E, Sosnik R, Bagdasarian K, Haidarliu S (2001) Temporal frequency of whisker movement. II. Laminar organization of cortical representations. J Neurophysiol 86:354–367

Arabzadeh E, Petersen RS, Diamond ME (2003) Encoding of whisker vibration by rat barrel cortex neurons: implications for texture discrimination. J Neurosci 23:9146–9154

Armstrong-James M, Fox K (1987) Spatiotemporal convergence and divergence in the rat SI "barrel" cortex. J Comp Neurol 263:265–281

Armstrong-James M, George MJ (1988) Influence of anesthesia on spontaneous activity and receptive field size of single units in rat SmI neocortex. Exp Neurol 99:369–387

Armstrong-James M, Diamond ME, Ebner FF (1994) An innocuous bias in whisker use in adult rats modifies receptive fields of barrel cortex neurons. J Neurosci 14:6978–6991

Berg RW, Kleinfeld D (2003) Rhythmic whisking by rat: retraction as well as protraction of the vibrissae is under active muscular control. J Neurophysiol 89:104–117

Brecht M, Sakmann B (2002) Dynamic representation of whisker deflection by synaptic potentials in spiny stellate and pyramidal cells in the barrels and septa of layer 4 rat somatosensory cortex. J Physiol 543:49–70

Brett-Green B, Paulsen M, Staba RJ, Fifkova E, Barth DS (2004) Two distinct regions of secondary somatosensory cortex in the rat: topographical organization and multisensory responses. J Neurophysiol 91:1327–1336

Brumberg JC, Pinto DJ, Simons DJ (1999) Cortical columnar processing in the rat whisker-to-barrel system. J Neurophysiol 82:1808–1817

Burton H, Mitchell G, Brent D (1982) Second somatic sensory area in the cerebral cortex of cats: somatotopic organization and cytoarchitecture. J Comp Neurol 210:109–135

Carvell GE, Simons DJ (1986) Somatotopic organization of the second somatosensory area (SII) in the cerebral cortex of the mouse. Somatosens Res 3:213–237
Carvell GE, Simons DJ (1987) Thalamic and corticocortical connections of the second somatic sensory area of the mouse. J Comp Neurol 265:409–427
Carvell GE, Simons DJ (1990) Biometric analysis of vibrissal tactile discrimination in the rat. J Neurosci 10:2638–2684
Carvell GE, Simons DJ (1995) Task and subject related differences in sensorimotor behavior during active touch. Somatosens Mot Res 12:1–9
Cascio CJ, Sathian K (2001) Temporal cues contribute to tactile perception of roughness. J Neurosci 21:5289–5296
Castro-Alamancos MA (2004) Absence of rapid sensory adaptation in neocortex during information processing states. Neuron 41:455–464
Castro-Alamancos MA, Oldford E (2002) Cortical sensory suppression during arousal is due to the activity-dependent depression of thalamocortical synapses. J Physiol 541:319–331
Champney G, Sachdev R, Maguire M, Melzer P, Ebner F (2001) Neural encoding of frequency of whisker stimulation in S1 and S2 is influenced by callosal input. Soc Neurosci Abstr 27:51.11
Chmielowska J, Carvell GE, Simons DJ (1989) Spatial organization of thalamocortical and corticothalamic projection systems in rat SmI barrel cortex. J Comp Neurol 285:325–338
Chung S, Li X, Nelson SB (2002) Short-term depression at thalamocortical synapses contributes to rapid adaptation of cortical sensory responses in vivo. Neuron 34:437–446
Derdikman D, Hildesheim R, Ahissar E, Arieli A, Grinvald A (2003) Imaging spatiotemporal dynamics of surround inhibition in the barrels somatosensory cortex. J Neurosci 23:3100–3105
Detre JA, Ances BM, Takahashi K, Greenberg JH (1998) Signal averaged laser Doppler measurements of activation-flow coupling in the rat forepaw somatosensory cortex. Brain Res 796:91–98
Diamond ME, Armstrong-James M, Ebner FF (1992) Somatic sensory responses in the rostral sector of the posterior group (Pom) and in the ventral posterior medial nucleus (VPM) of the rat thalamus. J Comp Neurol 318:462–476
Dörfl J, Welker E, Melzer P, Van der Loos H (1988) Left–right interactions determine the central effect of whisker clipping in the adult mouse; a deoxyglucose study. Soc Neurosci Abstr 14:424
Dykes RW, Lamour Y (1988) An electrophysiological study of single somatosensory neurons in rat granular cortex serving the limbs: a laminar analysis. J Neurophysiol 60:703–724
Erchova IA, Lebedev MA, Diamond ME (2002) Somatosensory cortical neuronal population activity across states of anesthesia. Eur J Neurosci 15:744–752
Fabri M, Burton H (1991) Ipsilateral cortical connections of primary somatic sensory cortex in rats. J Comp Neurol 311:405–424
Fanselow EE, Nicolelis MAL (1999) Behavioral modulation of tactile responses in the rat somatosensory system. J Neurophysiol 19:7603–7616
Fee MS, Mitra PP, Kleinfeld D (1997) Central versus peripheral determinants of patterned spike activity in rat vibrissa cortex during whisking. J Neurophysiol 78:1144–1149
Fox K, Armstrong-James M (1986) The role of the anterior intralaminar nuclei and *N*-methyl D-aspartate receptors in the generation of spontaneous bursts in rat neocortical neurones. Exp Brain Res 63:505–518
Friedberg MH, Lee SM, Ebner FF (1999) Modulation of receptive field properties of thalamic somatosensory neurons by the depth of anesthesia. J Neurophysiol 81:2243–2252
Ganguly K, Kleinfeld D (2004) Goal-directed whisking increases phase-locking between vibrissa movement and electrical activity in primary sensory cortex in rat. Proc Natl Acad Sci USA 101:12348–12353
Gao P, Bermejo R, Zeigler HP (2001) Whisker deafferentation and rodent whisking patterns: behavioral evidence for a central pattern generator. J Neurosci 21:5374–5380
Garabedian CE, Jones SR, Merzenich MM, Dale A, Moore CI (2003) Band-pass response properties of rat SI neurons. J Neurophysiol 90:1379–1391
Ghazanfar AA, Nicolelis MA (1997) Nonlinear processing of tactile information in the thalamocortical loop. J Neurophysiol 78:506–510
Gopal KV, Gross GW (1996) Auditory cortical neurons in vitro: initial pharmacological studies. Acta Otolaryngol 116:697–704
Harris JA, Diamond ME (2000) Ipsilateral and contralateral transfer of tactile learning. Neuroreport 11:263–266
Hernández A, Zainos A, Romo R (2000) Neuronal correlate of sensory discrimination in the somatosensory cortex. Proc Natl Acad Sci USA 97:6191–6196
Hewson-Stoate N, Jones M, Martindale J, Berwick J, Mayhew J (2005) Further nonlinearities in neurovascular coupling in rodent barrel cortex. Neuroimage 24:565–574
Hutson KA, Masterton RB (1986) The sensory contribution of a single vibrissa's cortical barrel. J Neurophysiol 56:1196–1233
Ito M (1985) Processing of vibrissa sensory information within rat neocortex. J Neurophysiol 54:479–490
Johnson KO (1974) Reconstruction of population response to a vibratory stimulus in quickly adapting mechanoreceptive afferent fiber population innervating glabrous skin of the monkey. J Neurophysiol 37:48–72
Khatri V, Hartings JA, Simons DJ (2004) Adaptation in thalamic barreloid and cortical barrel neurons to periodic whisker deflections varying in frequency and velocity. J Neurophysiol 92:3244–3254
Kim U, Ebner FF (1999) Barrels and septa: separate circuits in rat barrel field cortex. J Comp Neurol 408:489–505
Kleinfeld D, Sachdev RN, Merchant LM, Jarvis MR, Ebner FF (2002) Adaptive filtering of vibrissa input in motor cortex of rat. Neuron 34:1021–1034
König P, Engel AK, Singer W (1996) Integrator or coincidence detector? The role of the cortical neuron revisited. Trends Neurosci 19:130–137
Koralek KA, Jensen KF, Killackey HP (1988) Evidence for two complementary patterns of thalamic input to the rat somatosensory cortex. Brain Res 463:346–351
Krubitzer LA, Sesma MA, Kaas JH (1986) Microelectrode maps, myeloarchitecture, and cortical connections of three somatotopically organized representations of the body surface in the parietal cortex of squirrels. J Comp Neurol 250:403–430
Krupa DJ, Matell MS, Brisben AJ, Oliveira LM, Nicolelis MA (2001) Behavioral properties of the trigeminal somatosensory system in rats performing whisker-dependent tactile discriminations. J Neurophysiol 21:5752–5763
Krupa DJ, Wiest MC, Shuler MG, Laubach M, Nicolelis MA (2004) Layer-specific somatosensory cortical activation during active tactile discrimination. Science 304:1989–1992
Levitt J, Levitt M (1968) Sensory hind-limb representation in SmI cortex of the cat. Exp Neurol 22:259–275
Li L, Rema V, Ebner FF (2005) Chronic suppression of activity in barrel field cortex downregulates sensory responses in contralateral barrel field cortex. J Neurophysiol 94:3342–3356
Lu SM, Lin RC (1993) Thalamic afferents of the barrel cortex: a light- and electron-microscopic study using *Phaseolus vulgaris* leucoagglutinin as an anterograde tracer. Somatosens Mot Res 10:1–16
McCormick DA, Connors BW, Lighthall JW, Prince DA (1985) Comparative electrophysiology of pyramidal and sparsely spiny stellate neurons of the neocortex. J Neurophysiol 54:782–806
Melzer P, Ebner FF (2004) The BOLD response in somatic sensory cortex peaks with multiple whisker stimulation at low whisk rates: a functional magnetic resonance imaging study without anesthesia. Soc Neurosci Abstr 30:977.4
Mineo L, Melzer P, Ebner F (2002) Whisk rate of blind rats is accelerated during object discrimination. Soc Neurosci Abstr 28:257.9
Mirabella G, Battiston S, Diamond ME (2001) Integration of multiple-whisker inputs in rat somatosensory cortex. Cereb Cortex 11:164–170

Moskalenko YE, Dowling JL, Liu D, Rovainen CM, Semernia VN, Woolsey TA (1996) LCBF changes in rat somatosensory cortex during whisker stimulation monitored by dynamic H2 clearance. Int J Psychophysiol 21:45–59

Moore CI, Nelson SB, Sur M (1999) Dynamics of neuronal processing in rat somatosensory cortex. Trends Neurosci 22:513–520

Mountcastle VB (1957) Modality and topographic properties of single neurons of cat's somatic sensory cortex. J Neurophysiol 20:408–434

Mountcastle VB, Talbot WH, Darian-Smith I, Kornhuber HH (1967) Neural basis of the sense of flutter-vibration. Science 155:597–600

Mountcastle VB, Talbot WH, Sakata H, Hyvärinen J (1969) Cortical neuronal mechanisms in flutter-vibration studied in unanesthetized monkeys. Neuronal periodicity and frequency discrimination. J Neurophysiol 32:453–484

Ngai AC, Jolley MA, D'Ambrosio R, Meno JR, Winn HR (1999) Frequency-dependent changes in cerebral blood flow and evoked potentials during somatosensory stimulation in the rat. Brain Res 837:221–228

Perkel DH, Gerstein GL, Moore GP (1967) Neuronal spike trains and stochastic point processes. II. Simultaneous spike trains. Biophys J 4:419–440

Pidoux B, Verley R (1979) Projections on the cortical somatic I barrel subfield from ipsilateral vibrissae in adult rodents. Electroencephalogr Clin Neurophysiol 46:715–726

Pierret T, Lavallée P, Deschênes M (2000) Parallel streams for the relay of vibrissal information through thalamic barreloids. J Neurosci 20:7455–7462

Pruett JR Jr, Sinclair RJ, Burton H (2000) Response patterns in second somatosensory cortex (SII) of awake monkeys to passively applied tactile gratings. J Neurophysiol 84:780–797

Remple MS, Henry EC, Catania KC (2003) Organization of somatosensory cortex in the laboratory rat (*Rattus norvegicus*): evidence for two lateral areas joined at the representation of the teeth. J Comp Neurol 467:105–118

Romo R, Hernández A, Zainos A, Lemus L, Brody CD (2002) Neuronal correlates of decision-making in secondary somatosensory cortex. Nat Neurosci 5:1217–1225

Rose JE, Hind JE, Anderson DJ, Brugge JF (1971) Some effects of stimulus intensity on response of auditory nerve fibers in the squirrel monkey. J Neurophysiol 34:685–699

Salinas E, Hernández A, Zainos A, Romo R (2000) Periodicity and firing rate as candidate neural codes for the frequency of vibrotactile stimuli. J Neurosci 20:5503–5515

Shimegi S, Ichikawa T, Akasaki T, Sato H (1999) Temporal characteristics of response integration evoked by multiple whisker stimulations in the barrel cortex of rats. J Neurosci 15:10164–10175

Shimegi S, Akasaki T, Ichikawa T, Sato H (2000) Physiological and anatomical organization of multiwhisker response interactions in the barrel cortex of rats. J Neurosci 20:6241–6248

Shuler MG, Krupa DJ, Nicolelis MA (2001) Bilateral integration of whisker information in the primary somatosensory cortex of rats. J Neurosci 21:5251–5261

Silva AC, Lee SP, Yang G, Iadecola C, Kim SG (1999) Simultaneous blood oxygenation level-dependent and cerebral blood flow functional magnetic resonance imaging during forepaw stimulation in the rat. J Cereb Blood Flow Metab 19:871–879

Simons DJ (1978) Response properties of vibrissa units in rats SI somatosensory neocortex. J Neurophysiol 41:798–820

Simons DJ (1983) Multi-whisker stimulation and its effects on vibrissa units in rat SmI barrel cortex. Brain Res 276:178–182

Simons DJ, Carvell GE, Hershey AE, Bryant DP (1992) Responses of barrel cortex neurons in awake rats and effects of urethane anesthesia. Exp Brain Res 91:259–272

Sinclair RJ, Burton H (1991) Neuronal activity in the primary somatosensory cortex in monkeys (*Macaca mulatta*) during active touch of textured surface gratings: responses to groove width, applied force, and velocity of motion. J Neurophysiol 66:153–169

Spreafico R, Barbaresi P, Weinberg RJ, Rustioni (1987) A SII-projecting neurons in the rat thalamus: a single- and double-retrograde-tracing study. Somatosens Res 4:359–375

Swadlow HA (1989) Efferent neurons and suspected interneurons in S-1 vibrissa cortex of the awake rabbit: receptive fields and axonal properties. J Neurophysiol 62:288–308

Swadlow HA (1991) Efferent neurons and suspected interneurons in second somatosensory cortex of the awake rabbit: receptive fields and axonal properties. J Neurophysiol 66:1392–1409

Ureshi M, Matsuura T, Kanno I (2004) Stimulus frequency dependence of the linear relationship between local cerebral blood flow and field potential evoked by activation of rat somatosensory cortex. Neurosci Res 48:147–153

Vincent SB (1912) The function of the vibrissa in the behavior of the white rat. Behav Monogr 1:7–86

Vogel J, Kuschinsky W (1996) Decreased heterogeneity of capillary plasma flow in the rat whisker-barrel cortex during functional hyperemia. J Cereb Blood Flow Metab 16:1300–1306

Wallace MT, Ramachandran R, Stein BE (2004) A revised view of sensory cortical parcellation. Proc Natl Acad Sci USA 101:2167–2172

Welker C, Sinha MM (1972) Somatotopic organization of SmII cerebral neocortex in albino rat. Brain Res 37:132–136

Welker WI (1964) Analysis of sniffing of the albino rat. Behaviour 22:223–244

Whitsel BL, Kelly EF, Quibrera M, Tommerdahl M, Li Y, Favorov OV, Xu M, Metz CB (2003) Time-dependence of SI RA neuron response to cutaneous flutter stimulation. Somatosens Mot Res 20:45–69

Wong-Riley M (1979) Changes in the visual system of monocularly sutured or enucleated cats demonstrable with cytochrome oxidase histochemistry. Brain Res 171:11–28

Woolsey CN, LeMessurier DH (1948) The pattern of cutaneous representation in the rat's cerebral cortex. Fed Proc 7:137–138

Woolsey TA, Van der Loos H (1970) The structural organization of layer IV in the somatosensory region (S I) of mouse cerebral cortex. The description of a cortical field composed of discrete cytoarchitectonic units. Brain Res 17:205–242

Zhang HQ, Zachariah MK, Coleman GT, Rowe MJ (2001) Hierarchical equivalence of somatosensory areas I and II for tactile processing in the cerebral cortex of the marmoset monkey. J Neurophysiol 85:1823–1835